Neurochemistry International 129 (2019) 104476

Contents lists available at ScienceDirect

Neurochemistry International

journal homepage: www.elsevier.com/locate/neuint

Effects of exercise-induced fatigue on the morphology of asymmetric synapse and synaptic protein levels in rat striatum

Zhifeng Wang[a], Lijuan Hou[b], Dongmei Wang[c,*]

[a] Department of Physical Education, Xi'an Polytechnic University, Xi'an, Shanxi, 710048, China
[b] Physical Education and Sports College, Beijing Normal University, Beijing, 100875, China
[c] College of Sports Medicine and Rehabilitation, Shandong First Medical University & Shandong Academy of Medical Sciences, Tai'an, Shandong, 271000, China

ARTICLE INFO

Keywords:
Exercise-induced fatigue
Rat
Striatum
Asymmetric synapse
Synaptic protein
Ultrastructure

ABSTRACT

Corticostriatal synaptic plasticity is considered to be a cellular basis for somatic motor regulation and motor skill learning. Changes in synaptic transmission efficiency underlie functional plasticity, while structural plasticity involves changes in the ultrastructure of the synapse and the levels of synaptic proteins. Exercise-induced fatigue may impair corticostriatal synaptic plasticity, and this impairment may be an important mechanism for exercise-induced fatigue. However, prior research focused mainly on functional plasticity such that the structural plasticity was not well understood. Because corticostriatal synapses are typical asymmetric synapses, here we have used transmission electron microscopy to examine the changes of asymmetry synaptic ultrastructure in rat striatum before and after repetitive exercise-induced fatigue; we have also used western blotting to detect the levels of synaptic active region protein Munc 13, RIM1 and synaptic vesicle protein Rab3A and postsynaptic density PSD-95 protein in rat striatum before and after exercise-induced fatigue. The results showed that the ultrastructure of asymmetry corticostriatal synapses and synaptic protein levels in the striatum of rats were abnormally changed after repetitive exercise-induced fatigue. These abnormal changes in synaptic ultrastructure and related protein levels may be the structural basis for the corticostriatal plasticity impairment after exercise-induced fatigue.

1. Introduction

Exercise-induced fatigue can be divided into peripheral fatigue and central fatigue. Peripheral fatigue occurs at the peripheral muscle or neuromuscular junction, and central fatigue limits the factors that induce fatigue to the central nervous system (Meeusen et al., 2006). Studies have shown that the central nervous system plays a leading role in the occurrence of exercise-induced fatigue (Secher et al., 2006), and the decline in motor ability during exercise is due to fatigue in the central nervous system (Davis and Bailey, 1997; Davis et al., 2000; Meeusen et al., 2007). The basal ganglia, a group of interconnected subcortical nuclei, plays a prominent role in central fatigue regulation (Nakagawa et al., 2016; Chaudhuri and Behan, 2000). Striatum is the main input nucleus of the basal ganglia. Magnetic Resonance Imaging (MRI) found abnormal changes in the activity of the striatum during human fatigue, and it is suggested that this abnormal activity is related to fatigue (DeLuca et al., 2009), but the specific neural and molecular mechanisms have not been elucidated.

As a major input nucleus, the striatum receives glutamatergic projections from the cortex and thalamus as well as dopaminergic projections from the compact region of the substantia nigra (Smith et al., 2004; Ding et al., 2008; Zhai et al., 2018). According to the function and nerve fiber projections, the striatum can be divided into dorsomedial striatum (DMS) and dorsolateral striatum (DLS) (Poldrack and Packard, 2003; Takakusaki et al., 2004; Yin et al., 2006). DMS mainly receives glutamatergic projections from prefrontal cortex and plays an important role in the acquisition and execution of target-directed behavior (Shiflett and Balleine, 2011), while DLS mainly receives glutamatergic projections from primary motor cortex and sensorimotor area, and participates in the regulation of voluntary movement, motor skill learning and habitual behavior (Di Filippo et al., 2009; Alloway et al., 2006). The corticostriatal synapses are typical asymmetric synapses that can undergo plasticity changes, and this plasticity is considered to be an important cellular basis for motor learning, habit formation and somatic motor regulation (Milosevic et al., 2018; Yin and Knowlton, 2006). Abnormal corticostriatal synaptic plasticity is not only an important pathological mechanism leading to Parkinson's disease (Picconi et al., 2012; Paillé et al., 2010), Huntington's disease

* Corresponding author.
E-mail address: wangdm72@126.com (D. Wang).

https://doi.org/10.1016/j.neuint.2019.104476
Received 3 January 2019; Received in revised form 20 April 2019; Accepted 26 May 2019
Available online 27 May 2019

(Dalbem et al., 2005; Picconi et al., 2006) and dystonia (Martella et al., 2009), but also one of the important factors of exercise-induced fatigue (Ma et al., 2018).

Corticostriatal synaptic plasticity includes functional plasticity and structural plasticity. Long-term potentiation and long-term depression are the main forms of synaptic functional plasticity (Partridge et al., 2000; Ronesi and Lovinger, 2005), while synaptic structural plasticity mainly includes changes in dendritic spine numbers of striatal medium spiny neurons (Petzinger et al., 2007), the thickness of postsynaptic density (PSD), the change of the number and proportion of perforated synapses (Smith et al., 2009; Nezhadi et al., 2017) and changes in the levels of synaptophysin (Bai and Strong, 2014), RIM1, Munc13 (García-Junco-Clemente et al., 2005) and Rab3A (Sakane et al., 2006). Human experiments show that proper physical exercise is conductive to maintain brain health, synaptic plasticity and cognitive function (Cotman and Berchtold, 2002; Fernandes et al., 2017). Animal experiments also show that voluntary exercise can increase the regeneration of brain neurons, reduce injury, improve neuroplasticity and cognitive function (Carro et al., 2001; van Praag et al., 1999). However, prolonged and intensive exercise not only reduces motor function (Aune et al., 2008), but also impairs synaptic plasticity and cognition, including information processing and decision making (Thomson et al., 2009; Moore et al., 2012). Animal experiments have also confirmed that high intensity treadmill exercise can reduce the spatial memory ability of mice and impair synaptic functional plasticity in the hippocampus (Sun et al., 2017) and striatum (Ma et al., 2018). The integrity of corticostriatal synaptic structure is the basis for maintaining its normal function. However, it is unclear whether the corticostriatal functional plasticity impairment is accompanied by changes in morphology and related protein levels after intensive exercise.

In this paper, we used transmission electron microscopy and western blotting to study corticostriatal synapses after exercise-induced fatigue in rats.

2. Materials and methods

2.1. Experimental animals and groups

Seventy-two adult male Wistar rats (body weight 300–320g) were used in the experiment. The experimental animals were purchased from Beijing Weitonglihua Experimental Animal Technology Co., Ltd. China, and the production license was SCXK (Beijing) 2016-0011. Food and water were provided ad libitum. The temperature of the animal room was controlled at 20–25 °C, and the humidity was kept at 45%–50%. Three days later, rats were randomly divided into 6 groups: quiet control group (CG, n = 12), 1d fatigue group (1FG, n = 12), 3d fatigue group (3FG, n = 12), 7d fatigue group (7FG, n = 12), 12-h recovery group after 7d fatigue (12RG, n = 12) and 24-h recovery group after 7d fatigue (24RG, n = 12). Behavioral tests were performed immediately after successful model establishment. Afterwards, rats in each group were randomly divided into two subgroups, 6 rats in each group, and brain tissues of these rats were subjected to transmission electron microscopy and western blotting.

2.2. Experimental instruments and reagents

Main experimental instruments: animal treadmill (DSPT-202, HangZhouDuanShi, China), paraffin slicer (RM2235, Leica, Germany), image analyzer (Leica-200, Germany), transmission electron microscope (Hitachi H-7650, Japan), electric heating incubator (DNP-9802, ShanghaiJinghong Laboratory Instrument Co., Ltd., Shanghai, China), dehydrator (Thermo, Excelsior ES, USA), grip strength meter (BIO-GS3, Bioseb, Vitrolles, France), rotarod tester (Rotamex-5 RotaRod, USA).

Main experimental reagents: chloral hydrate (Sigma, USA), paraformaldehyde (Sigma, USA), anti-PSD-95 antibody (ab18258, Abcam, USA), anti-Munc13 antibody (Rb1242-051209-ws, Osense, Australia), anti-Rab3A antibody (ab3335, Abcam, USA), anti-RIM1 antibody (24576-1-AP, Proteintech, USA), Goat Anti-rabbit IgG/HRP and β-actin (bs-0295G-HRP, bs-0061R, Boosen Biological Technology Co., Ltd., Beijing, China).

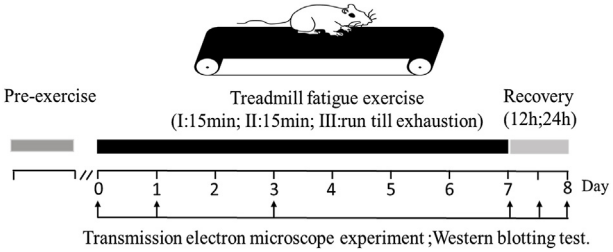

Fig. 1. Schematic illustration of establishing exercise-induced fatigue protocol.

2.3. The model of exercise-induced fatigue

Following published methods (Hu et al., 2015), the rats were placed on the treadmill for 30 min to familiarize themselves with the running environment, and then the treadmill running began. The exercise loading was classified into three stages: I: 10 m/min, 15min; II: 15 m/min, 15min; III: 20 m/min, run till exhaustion (Fig. 1). Criteria of exhaustion was as follows: the running posture changed from stomp-style into prostrate-style, and it remained stationary in the rear part of the treadmill, sound/light/electric stimulation could not keep it running.

2.4. Behavioral tests

Grip strength test. The maximal grip strength of rats was monitored using a grip strength meter, and the test can be used to assess the neuromuscular function of rats, mainly to measure the maximal muscle strength of forelimbs. When the tester grabs the tail of the rat and pulls it back, the rat will instinctively grab the grip rod in front. When the tension of the tester exceeds the maximal grip strength of the rat, the rat will release the grip rod. At this time the instrument will automatically record and display the maximal grip value. Each rat was tested three times and the average value was obtained. Relative maximal grip strength (reflecting maximal strength) = maximal grip strength/body weight.

Rotarod test. This test evaluates motor balance and coordination as well as motor learning. In the rat, both aspects are under the control of the dopaminergic innervation of the dorsal striatum: the dorsomedial part controls motor learning and the dorsolateral part controls motor coordination and balance (Durieux et al., 2012; Voorn et al., 2004). Motor performance of rodents in the rotarod allows for reflecting the functional status of striatal neurons, and this has been used in the evaluation of motor dysfunction in PD (Rozas et al., 1998). The rotarod consists of a four-lane rotating rod (diameter 7.5 cm) and infrared beams to detect the moment of fall. The body of the rat was placed perpendicular to the rotating axis and the head against the direction of the rotation; the animal must therefore move forward to stay on the rod. Since several rats were generally tested in the same session, each rat rested for about 3 min between the different testing speeds. The rats were trained once on the rotarod at the constant speed of 10 rpm for 2 min during three consecutive days before the evaluation of their performance. In the evaluating session, the rats were placed on the rod and their performance was tested at different constant speeds (5, 10, 15 and 20 rpm) for a maximum of 2 min at each speed. All rats were video-recorded while staying on the rod to assess the qualitative aspect of recovery of motor coordination and posture.

2.5. Preparation of electron microscopy specimen

Rats in CG, FG and RG were anesthetized by intraperitoneal

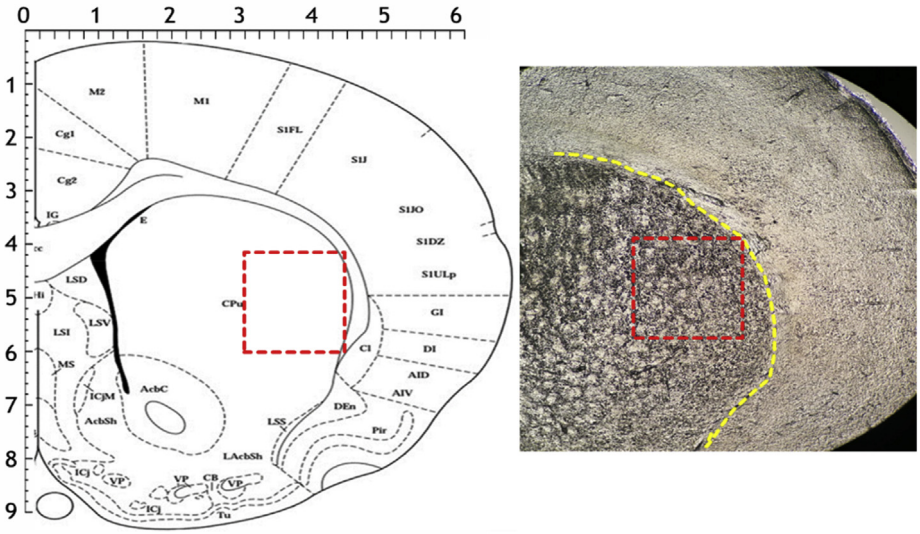

Fig. 2. Photograph area. Note: The left side is a coronal section of the right hemisphere of the rat brain. The right side is the right hemisphere slice of the rat brain. Red square is the photograph area.

injection of 10% chloral hydrate (3.5 ml/kg) during the corresponding period after fatiguing exercise. 0.1 mol/L PBS (including 100IU/mL heparin) at 37 °C and 4% paraformaldehyde containing 2% glutaraldehyde at 4 °C (prepared with 0.1 mol/L PBS, pH7.4) were perfused and fixed by left ventricular-ascending aorta intubation. One cubic millimeter of striatum was taken and fixed in 3% glutaraldehyde for 3 h. After immersion in 0.1 mol/L PBS for 10 min × 3 times, the striatum tissue was placed in 1% osmic acid (prepared with 0.1 mol/L PBS) for 40min. After dehydration and resin embedding, ultrathin sections of 70 nm thickness were cut and then counterstained with acetyl uranium and lead acetate.

2.6. Transmission electron microscopy

Tissue was examined under a Hitachi H-7650 Transmission Electron Microscope operated at 100 kV. Photographing the dorsolateral striatum (Fig. 2). Images were obtained at 40,000x magnification using an AMT digital camera and software. Three consecutive slices were cut at the same position of each rat's striatum for a total of 108 slices. For each striatum under investigation, a total of 40 images of simple, asymmetric synapses were obtained. Three synapses were imaged from each grid. Synapses were spaced by a minimum of one grid box to reduce bias. The microscopist was blinded to treatment conditions while imaging.

2.7. Transmission electron microscopy image analysis

Since the glutamatergic synapses of corticostriatal are mainly asymmetric synapses, the synapses that release GABA, DA and ACh are mainly symmetric synapses (Bamford et al., 2004; Kawaguchi, 1997; Izzo and Bolam, 1988), the asymmetric synapses were selected and taken photograph according to the random principle. Identification of neuronal ultrastructure follows published methods (Peters, 1991): The dendritic stems are nucleus-free protrusions with a smooth outline containing mitochondria, Nissl bodies and parallel neurofibrils, but no Glogi complexes. Dendritic spines are smaller than dendritic trunks, lacking microtubules, mitochondria and rough endoplasmic reticulum, and there are villous substances which often contain granular clusters. In some ultrathin slices, the head or/and neck of dendritic spine have spinous organs (flat membrane sac of endoplasmic reticulum). There are at least three synaptic vesicles in the presynaptic endings of asymmetric synapses with parallel antecedent membranes and a large gap between the anterior and posterior membranes and thicker PSD. The length of synaptic active zone, the thickness of PSD, the width of synaptic gap and the curvature of synaptic interface (i.e., the arc length/chord length of postsynaptic membrane) were measured by Leica-200 image analyzer (Güldner and Ingham, 1980; Kobayashi et al., 2014). The length of synaptic active zone and the thickness of PSD were measured following published method of Güldner and Ingham (1980), the curvature of synaptic interface was measured following the method of Jones and Devon (1978) and the width of synaptic gap was measured by multi-point averaging method. The center of the synaptic vesicles was labeled by point tools of Image Tool software (UTHSCSA, ImageTool, Version 3.0), the shortest distance between synaptic vesicles and presynaptic active zone and the shortest distance between synaptic vesicles were measured by LoClust software (Nikonenko and Skibo, 2004). If the synaptic vesicle contacts with the presynaptic active zone, it is defined as a releasing/docking vesicle; if the distance between the center of synaptic vesicle and the presynaptic active zone is less than 200 nm, it is defined as a recycling vesicle; if more than 200 nm, it is defined as resting vesicle pool (Zhang et al., 2015).

2.8. Western blotting

After behavioral testing was completed, the rats were anesthetized with 10% chloral hydrate (3.5 mL/kg), then were quickly decapitated, then the right striatum was separated on an ice tray and placed in a pre-cooled mortar. After adding the tissue lysate, the striatum was grinded and homogenized, then transferred to an EP tube, centrifuged at 14,000 rpm for 5 min, and the supernatant was collected. After the protein level was determined by BCA method, 5 times SDS was added, boiled for 5 min, cooled and stored in −80 °C refrigerator to be tested. Samples containing 20 μg total protein were selected for electrophoresis (S1: 90V, 15min; S2: 120V, to the end), followed by transfer to polyvinylidene fluoride (PVDF) membranes (100V, 90min). The PVDF membrane was immersed in 5% milk for 1 h and then added primary antibody (PSD, 1:1000; Rab3A, 1:1000; Munc13, 1:1000; RIM1, 1:500; β-actin, 1:200), incubated overnight at 4 °C. Wash 3 times with 1*TBST for 10min each time. The secondary antibody (Goat Anti-rabbit IgG/HRP, 1:1500) was added and incubated for 60 min at room

temperature, washed the membrane. ECL luminescent agent was added to the film and incubated at room temperature for 5min. After development and exposure, the gel imaging system (ChemiDoc MP) was used to photograph. The target protein was analyzed by image analysis software (Image J), target protein level = gray value of target protein/gray value of internal reference protein.

2.9. Statistical analysis

The experimental data were analyzed by SPSS 20.0 statistical software (IBM Corp., Armonk, NY, USA). Statistical data are expressed as mean ± standard deviation. One-way ANOVA was used to compare the differences between groups, then post hoc test was carried out. Under the circumstance of equal variances assumed, LSD was used to compare the homogeneity of variance, and when the variance was unequal, Tanhane's method was used to compare the differences. The differences were considered statistically significant when $P < 0.05$.

3. Results

3.1. Changes of body weight and behavior after exercise-induced fatigue

Behavioral observation showed that rats adjusted themselves well to the treadmill exercise at the beginning; rats were always in the middle or first 1/3 of the runway. Gradually, the exercise capacity of the rats decreased and they showed difficulty in maintaining the preconditioned speed, and running posture changed from stomp-style into prostrate-style, remaining stationary in the rear part of the treadmill, slight sound, light or direct current stimulation couldn't keep the rats running, and appeared fatigue state consistent with the literature (Hu et al., 2015). (Fig. 1).

All rats were weighed after treadmill exercise, and the results showed that the weight of rats decreased in varying degrees with the number of exercise fatigue increased, and there were significant differences between groups (one-Way ANOVA, df = 5, F = 10.30, P = 0.000). Post hoc test showed that 3FG was significantly lower than CG (n = 6, one-way ANOVA, P < 0.05). 7FG was significantly lower than CG and 1FG (n = 6, one-Way ANOVA, both P < 0.01). 12RG and 24RG were significantly lower than CG and 1FG (both n = 6, one-Way ANOVA, and the best P < 0.01), but there was no significant difference compared with 7FG (both n = 6, one-Way ANOVA, both P > 0.05). Weight loss in rats may be related to higher energy consumption during exercise (Fig. 3).

The results of relative grip strength after exercise-induced fatigue showed that relative grip strength of rats was significantly different among different groups (one-way ANOVA, df = 5, F = 117.28, P = 0.000). The results of post hoc test showed that the relative grip strength of rats in 1FG, 3FG and 7FG decreased significantly compared with CG (all n = 6, one-way ANOVA, all P < 0.01). The relative grip strength of 7FG was significantly lower than that of 1FG and 3FG (both P < 0.01). Both 12RG and 24RG showed a significant increase compared with 7FG (one-Way ANOVA, both P < 0.01), but still remained lower than CG (one-way ANOVA, both P < 0.01) (Fig. 4). The results suggest that exhaustive exercise can impair neuromuscular function and reduce muscle strength, which is consistent with reports by Park SS et al. (Park et al., 2019).

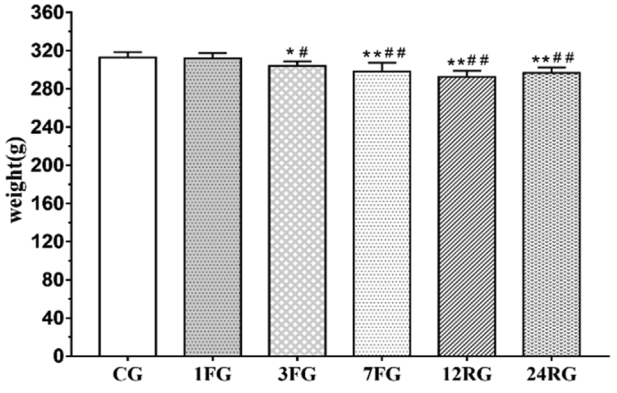

Fig. 3. Changes in body weight of rats in each group after exercise-induced fatigue Compared to CG, *:$P < 0.05$, **:$P < 0.01$; Compared to 1FG, #: $P < 0.05$, ##$P < 0.01$; Compared to 7FG, &:$P < 0.05$, &&:$P < 0.01$; Compared to 12RG, $:$P < 0.05$, $$:$P < 0.01$; (one-way analysis of variance).

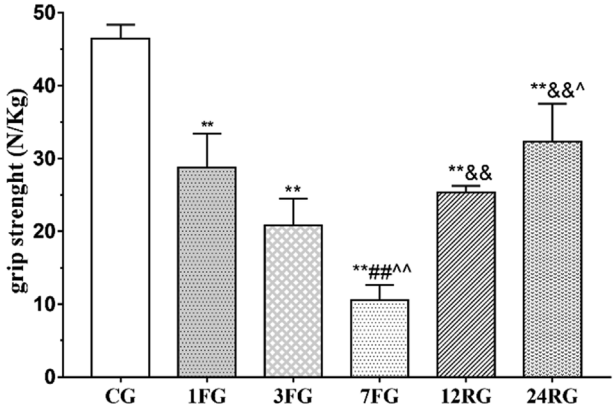

Fig. 4. Comparison of relative grip strength of rats in each group after exercise-induced fatigue. Compared to CG, *:$P < 0.05$, **:$P < 0.01$; Compared to 1FG, #: $P < 0.05$, ##$P < 0.01$; Compared to 3FG, ^:$P < 0.05$, ^^:$P < 0.01$; Compared to 7FG, &:$P < 0.05$, &&:$P < 0.01$; Compared to 12RG, $:$P < 0.05$, $$:$P < 0.01$; (one-way analysis of variance).

The balance ability and coordination of the rats after exercise-induced fatigue were further tested by rotarod test, the main observation index was the time that the rats stayed on the rotating rod at different rotational speeds (5, 10, 15 and 20 rpm). The comparison between groups showed that there were significant differences in the time staying on the rotating rod at 5, 10, 15 and 20 rpm (one-way ANOVA, all df = 5, respectively F = 10.88, 39.69, 58.01, 119.41, all P = 0.000). The results of post hoc test showed that the retention time in 7FG was significantly lower than that in CG at 5 rpm (n = 6, one-way ANOVA, P < 0.01). Compared with CG, the rest groups had a decreasing trend (all n = 6, one-way ANOVA, all P > 0.05).

The retention time of rats in 1FG, 3FG and 7FG was significantly lower than that in CG at the rotational speeds of 10 rpm, 15 rpm and 20 rpm (n = 6, one-way ANOVA, all P < 0.01). And the retention time of rats in 12RG and 24RG increased significantly compared with that in 7FG (n = 6, one-Way ANOVA, P < 0.05 or P < 0.01), but it was still significantly lower than that in CG (n = 6, one-way ANOVA, all P < 0.01) (Fig. 5). The results suggest that exercise-induced fatigue reduced the balance and coordination ability of rats, which is consistent

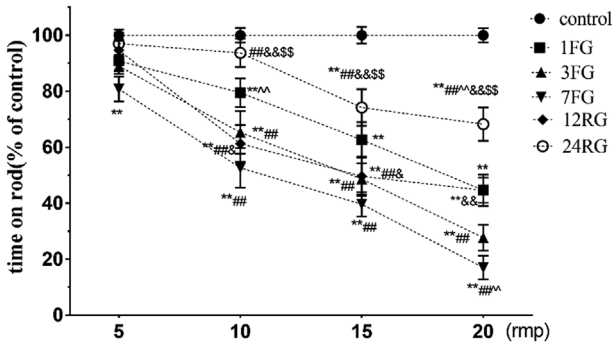

Fig. 5. Comparison of retention time of rats on the rotating rod in each group after exercise-induced fatigue.

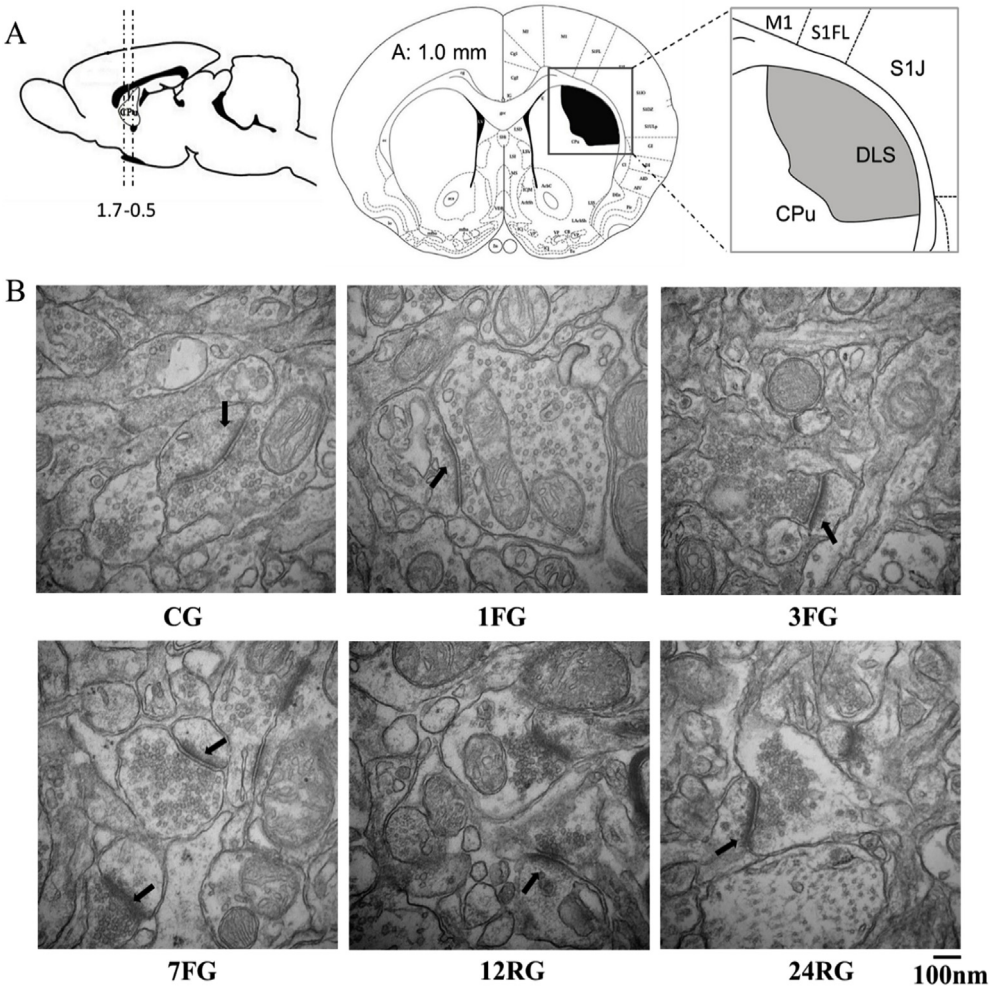

Fig. 6. Transmission electron microscopic observation of asymmetrical synapses in rat striatum in each group. A: Section of dorsolateral striatum and photographing site. B: Ultrastructural observation of asymmetric synapses, the arrow shows the postsynaptic thickness.

with the results reported in the literature (Franzone and Reboani, 1977). After 12 h and 24 h recovery, the retention time increased significantly, and the balance ability was restored significantly, but still could not reach the normal state.

3.2. Ultrastructural changes of asymmetrical synapses in rat striatum after exercise-induced fatigue

A large number of symmetric and asymmetric synapses were examined in the striatum under the transmission electron microscope. The presynaptic and postsynaptic membranes of asymmetric synapses are parallel, and PSD is thick and obvious (Fig. 6). The presynaptic and postsynaptic membranes of the symmetric synapses are also parallel, but the PSD is not obvious and only shows slight thickening. According to these characteristics, the two types of synapses can be distinguished. Since the asymmetric synapses in the striatum are mainly glutamatergic synapses, the asymmetric synapses selected in this study are mainly glutamatergic synapses. A total of 272 asymmetric synapses were selected according to the random principle for observation, measurement and analysis. There are 48 in CG, 42, 45, 48, 40 and 49 in 1FG, 3FG, 7FG, 12RG and 24RG, respectively. Among the 272 synapses selected, 91.86% of the asymmetric synapses were located on dendritic spine and 8.14% of the asymmetric synapses were located on the dendritic trunk, and there was only one asymmetric synapse on each dendritic spine.

Statistical results (Fig.6, Table 1) showed that PSD thickness, the length of synaptic active zone and the synaptic interface curvature of rat striatum asymmetric synapses after exercise fatigue were significantly different between groups (one-Way ANOVA, all df = 5, respectively F = 23.8, 18.69, 10.68, all P = 0.000), there was no difference in the width of synaptic cleft between groups (df = 5, F = 1.89, P = 0.68). Post hoc test results showed that there was no significant change in the PSD thickness, the length of synaptic active zone and the synaptic interface curvature of DLS asymmetric synapses in 1FG rats compared with CG (one-Way ANOVA, All $P > 0.05$). PSD thickness and the synaptic interface curvature of the striatum asymmetric synapses in 3FG were significantly higher than those in CG and 1FG (one-Way ANOVA, both $P < 0.05$), the length of synaptic active zone and the width of synaptic cleft had no significant changes compared with CG (one-way ANOVA, both $P > 0.05$). PSD thickness and the synaptic interface curvature of DLS asymmetric synapses in 7FG rats were significantly higher than those in CG and 1FG (one-way ANOVA, all $P < 0.01$), the length of synaptic active zone was significantly longer than that in CG and 1FG (one-way ANOVA, both $P < 0.05$), and the width of synaptic cleft had an increasing trend compared with CG ($P > 0.05$). PSD thickness and the synaptic interface curvature of the DLS striatum asymmetric synapses in 12RG rats had a decreasing trend compared with 7RG (both $P > 0.05$), but were still higher than CG (one-Way ANOVA, both $P < 0.05$), the length of synaptic active zone and the width of synaptic cleft had a decreasing trend compared with 7RG (all $P > 0.05$). The synaptic interface curvature in 7FG was also significantly higher than that in 1FG ($P < 0.01$). PSD thickness and the length of synaptic active zone in DLS striatum of 24RG rats were

Table 1
Measurement of structural parameters of glutamatergic synapses in rat dorsolateral striatum in different groups ($\bar{X} \pm SD$, n = 6) .

	thickness of post-synaptic density (nm)	length of synaptic active zone (nm)	width of synaptic cleft (nm)	curvature of synaptic interface
CG	49.29 ± 12.24	279.58 ± 65.77	17.69 ± 5.95	1.21 ± 0.24
1FG	48.98 ± 14.43	281.48 ± 75.84	16.98 ± 9.78	1.28 ± 0.21
3FG	54.98 ± 15.03$^{*\#}$	284.69 ± 90.07	19.69 ± 7.95	1.39 ± 0.28$^{*\#}$
7FG	64.26 ± 16.77$^{**\#\#}$	298.46 ± 85.75$^{*\#}$	21.09 ± 10.18	1.47 ± 0.61$^{**\#\#}$
12RG	55.26 ± 18.07*	290.48 ± 80.74	20.65 ± 9.58	1.41 ± 0.51$^{*\#\#}$
24RG	51.59 ± 16.76$^{\&}$	281.59 ± 77.97$^{\&}$	18.69 ± 10.95	1.29 ± 0.34$^{\&\&\$\$}$

Compared to CG, *:$P < 0.05$, **:$P < 0.01$; Compared to 1FG, #: $P < 0.05$, ##$P < 0.01$; Compared to 7FG, &:$P < 0.05$, &&:$P < 0.01$; Compared to 12RG, $:$P < 0.05$, $$:$P < 0.01$; (one-way analysis of variance).

significantly lower than those of 7FG rats (one-way ANOVA, both $P < 0.05$), the synaptic interface curvature was significantly lower (one-way ANOVA, $P < 0.01$), meanwhile, the synaptic interface curvature of 24RG rats was also significantly lower than that of 12RG rats (one-way ANOVA, $P < 0.01$).

3.3. Distribution of asymmetric synaptic vesicles in rats striatum after exercise-induced fatigue

Neurotransmitters are stored in synaptic vesicles and the distribution of synaptic vesicles may affect the normal release of neurotransmitters in synaptic vesicles and the synaptic function. It has been found that exercise fatigue can change striatum synaptic function (Ma et al., 2018). However, it is not known at present whether this change in synaptic function is accompanied by changes in the distribution of synaptic vesicles. Therefore, the distribution of vesicles in asymmetric synaptic terminals of DLS in each group was observed by transmission electron microscopy (Fig. 7). We first classified the vesicles in the presynaptic terminals into three categories based on published methods (Zhang et al., 2015; Fowler and Staras, 2015): (1) docking vesicles: connected to presynaptic active zone; (2) Recycling vesicles: less than 200 nm away from presynaptic active zone; (3) resting vesicles: more than 200 nm away from presynaptic active zone. Statistical results (Table 2) showed that there was no difference in the total number of synaptic vesicles between groups after exercise fatigue (one-way ANOVA, df = 5, F = 0.42, P = 0.83). There were significant intergroup differences in the number of docking vesicles, resting vesicles and recycling vesicles (Table 2) (one-way ANOVA, all df = 5, respectively F = 28.41, 21.88, 19.68, all P = 0.000). Post hoc test results showed (Table 2) that the total number of asymmetric synaptic vesicles in 1FG, 3FG, 7FG, 12RG, and 24RG was not significantly different from that in CG (one-Way ANOVA, all $P > 0.05$). The number of docking vesicles and recycling vesicles in 1FG had an increased trend compared with that in CG (one-Way ANOVA, both $P > 0.05$), and the number of resting vesicles decreased but had no significant difference (one-Way ANOVA, $P > 0.05$). The number of docking vesicles and recycling vesicles in 3FG was significantly increased compared with those in CG (one-Way ANOVA, $P < 0.05$ and $P < 0.01$), the number of resting vesicles was significantly lower than that in CG (one-Way ANOVA, $P < 0.01$). In addition, the number of docking vesicles and recycling vesicles in 3FG was significantly higher than that in 1FG (one-Way ANOVA, both $P < 0.05$), while the number of resting vesicles was significantly lower than that in 1FG (one-way ANOVA, $P < 0.05$). The number of docking vesicles and recycling vesicles in 7FG were significantly increased compared with CG and 1FG (one-Way ANOVA, all $P < 0.01$), while the number of resting vesicles was significantly lower than that in CG and 1FG (one-Way ANOVA, all $P < 0.01$). The number of docking vesicles and recycling vesicles in 12RG were significantly reduced compared with those in 7FG (one-Way ANOVA, both $P < 0.05$), but still significantly higher than those in CG (one-Way ANOVA, $P < 0.05$ and $P < 0.01$), the number of resting vesicles in 12RG had an increased trend compared with that in 7FG (one-Way ANOVA, $P > 0.05$), but it was still significantly lower than that in CG (one-Way ANOVA, $P < 0.01$). In addition, the number of recycling vesicles in 12RG was significantly higher than that in 1FG (one-way ANOVA, $P < 0.01$), while the number of resting vesicles was significantly lower than that in 1FG (one-way ANOVA, $P < 0.01$). The number of docking vesicles and recycling vesicles in 24RG decreased significantly compared with those in 7FG (one-way ANOVA, both $P < 0.01$), which was also significant decreased compared with those in 12RG (one-way ANOVA, both $P < 0.05$). The number of resting vesicles in 24RG was significantly higher than that in 7FG (one-way ANOVA, $P < 0.05$), but it was still significantly lower than that in CG (one-way ANOVA, $P < 0.05$).

After statistics of the distance between synaptic vesicles and synaptic active zone, it was further found (Fig. 8) that the distribution of synaptic vesicles in asymmetric synapses of rat striatum in CG was dispersed, and the histogram of synaptic vesicles tended to be normally distributed. However, under the condition of exercise fatigue, especially after repetitive exercise fatigue, synaptic vesicles began to concentrate in the presynaptic active zone and the histogram showed a positive skewness distribution. These results suggest that repetitive exercise fatigue remodels the spatial distribution of synaptic vesicles in the striatum, and the final result is that asymmetric synaptic vesicles are

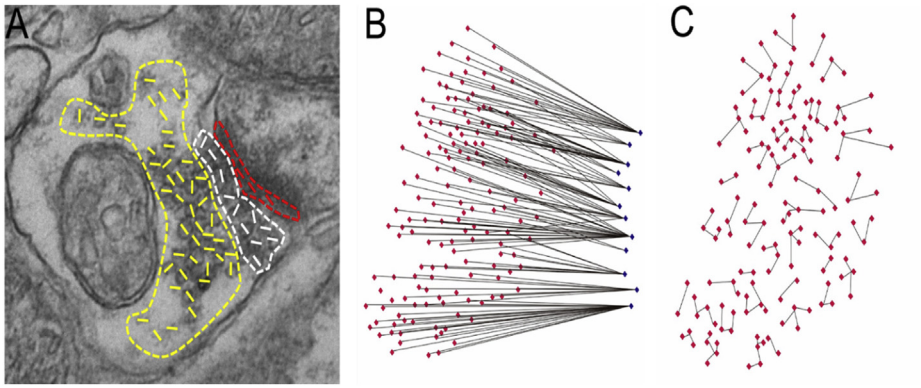

Fig. 7. Distribution of synaptic vesicles in asymmetric synapses of rat striatum(A) Asymmetric synaptic structure under electron microscope. Docking vesicles contact with the presynaptic active zone (PAZ), their diameter is marked in red. Recycling vesicles are those that are found within 200 nm from the PAZ, their diameter is marked in white. Resting vesicles are found more than 200 nm away from the PAZ, their diameter is marked in yellow. (B) Quantitative measurement of AZD using LoClust software. (C) Quantitative measurement of synaptic vesicle distance using LoClust software.

Table 2
Statistics on the number of asymmetric synaptic vesicles in DLS of rats in each group ($\bar{X} \pm SD$)

	Docked Vesicle Pool	Recycling Vesicle Pool	Resting Vesicle Pool	Total Number of Vesicles
CG	9.35 ± 1.53	22.20 ± 7.89	58.02 ± 10.81	97.68 ± 27.85
1FG	10.58 ± 1.43	26.02 ± 8.81	55.36 ± 10.15	101.66 ± 30.23
3FG	12.79 ± 2.03$^{*\#}$	32.35 ± 8.07$^{**\#}$	47.69 ± 9.95$^{**\#}$	103.09 ± 33.09
7FG	14.26 ± 2.12$^{**\#\#}$	40.82 ± 9.09$^{**\#\#}$	42.55 ± 8.64$^{**\#\#}$	110.49 ± 30.98
12RG	12.12 ± 1.87$^{*\&}$	34.07 ± 8.85$^{**\#\#\&}$	46.95 ± 9.31$^{**\#\#}$	99.41 ± 35.51
24RG	10.09 ± 1.66$^{\&\&\$}$	24.99 ± 9.19$^{\&\&\$}$	50.79 ± 10.95$^{*\&}$	102.87 ± 36.36

more likely to release neurotransmitters under exercise fatigue.

Statistical analysis of vesicle diameter and vesicle spacing showed that there were no differences in vesicle diameter of the docking vesicles, recycling vesicles and resting vesicles in the asymmetrical synapses of rat striatum after exercise fatigue (one-way ANOVA, all df = 5, respectively F = 0.47, 0.65, 0.55, respectively P = 0.85, 0.89,

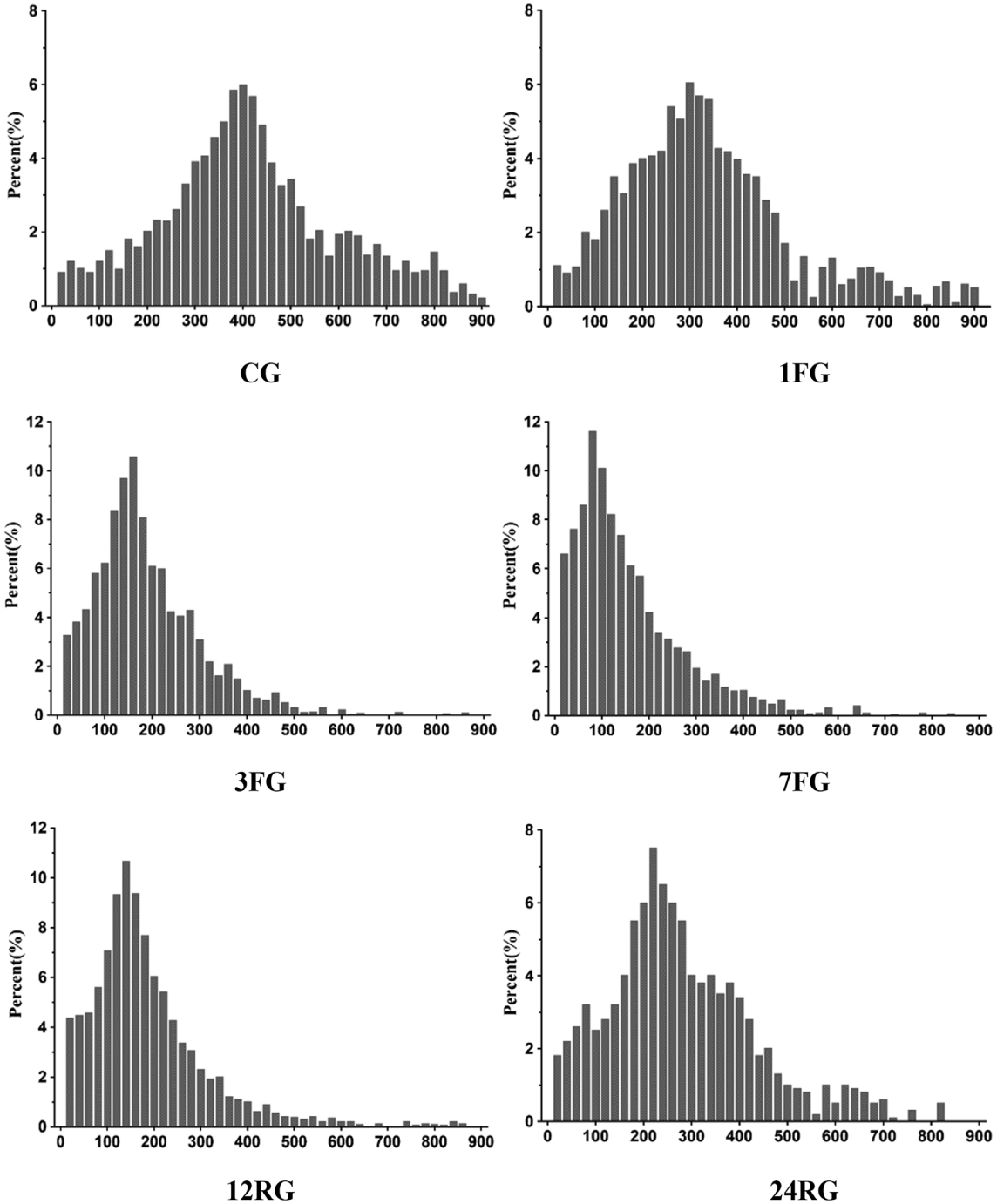

Fig. 8. Histogram of asymmetric presynaptic vesicles distribution in rat striatum in each group. Note: abscissa unit: nm.

Table 3
Diameter and nearest distance statistics of DLS asymmetric synaptic vesicles of rats in each group ($\bar{X} \pm SD$)

	Vesicular Diameters (nm)			Nearest Neighbor Distance (Clustering)	
	Docked Vesicle	Recycling Vesicle	Resting Vesicle	Resting (201–900 nm)	Docked + Recycling (0–200 nm)
CG	20.98 ± 1.31	23.79 ± 1.36	24.68 ± 1.51	42.41 ± 0.79	42.98 ± 0.75
1FG	21.09 ± 1.29	23.98 ± 1.41	24.32 ± 1.65	42.89 ± 0.85	42.24 ± 0.68
3FG	20.89 ± 1.64	24.32 ± 1.63	24.78 ± 1.59	43.95 ± 0.63$^{*\#}$	41.09 ± 0.81$^{*\#}$
7FG	20.78 ± 1.71	24.29 ± 1.81	25.06 ± 1.75	44.75 ± 0.88$^{**\#\#}$	40.08 ± 0.91$^{**\#\#}$
12RG	21.11 ± 1.27	24.81 ± 1.49	25.22 ± 1.22	44.09 ± 0.81$^{**\#}$	41.33 ± 0.75$^{*\#\&}$
24RG	20.33 ± 1.55	24.09 ± 1.82	24.69 ± 1.97	43.68 ± 0.84$^{*\&}$	41.89 ± 0.88$^{*\&}$

0.77), but the closest distance between resting vesicle and docking vesicle + recycling vesicle was significantly different among different groups (one-way ANOVA, both df = 5, respectively F = 8.67, 12.6, both P = 0.000) (Table 3).

The results of post hoc test showed that there was no significant change in the distance between the striatum asymmetric synaptic vesicles (including docking vesicles, recycling vesicles and resting vesicles) in 1FG compared with that in CG (one-Way ANOVA, all P > 0.05). The distance between resting vesicles in 3FG was significantly higher than that in CG and 1FG (one-Way ANOVA, both P < 0.05), the shortest distance between the docking vesicles and recycling vesicles was significantly lower than that in CG and 1FG (one-Way ANOVA, both P < 0.05). The distance between the resting vesicles in 7FG was higher than that in CG and 1FG (one-way ANOVA, both P < 0.01), the shortest distance between docking vesicles and recycling vesicles was significantly lower than that in CG and 1FG (one-way ANOVA, both P < 0.01). The distance between the resting vesicles in 12FG showed a decreasing trend compared with that in 7FG (one-Way ANOVA, P > 0.05), but remained significantly higher than that in 1FG and CG (one-Way ANOVA, P < 0.05 and P < 0.01). The shortest distance between striatal docking vesicles and recycling vesicles in 12RG was significantly increased compared with that in 7FG (one-Way ANOVA, P < 0.05), but remained significantly lower than 1FG and CG (one-Way ANOVA, both P < 0.05). The shortest distance between resting vesicles in 24RG was significantly lower than that in 7FG (one-Way ANOVA, P < 0.05), but it was still higher than that in CG (one-Way ANOVA, P < 0.05). The shortest distance between the striatal docking vesicles and recycling vesicles in 24RG was significantly increased compared with that in 7FG (one-Way ANOVA, P < 0.05), but it was still significantly lower than that in CG (one-Way ANOVA, P < 0.05). The results suggest that synaptic vesicles in striatal asymmetric synapses accumulate in the space near the synaptic active zone, making synaptic vesicles easier to dock and release, which may be an important sign of synaptic function enhancement.

3.4. Changes of synaptic protein levels in rat striatum after exercise-induced fatigue

The results of western blotting showed that the levels of PSD-95 (Fig. 9), Munc13 (Fig. 10) and Rab3A (Fig. 12) in rat striatum had extremely significant inter-group differences after exercise fatigue (one-way ANOVA, all df = 5, respectively F = 33.72, 45.58, 38.87, all P = 0.000), RIM1 (Fig. 11) had no inter-group differences (one-way ANOVA, df = 5, F = 1.26, P = 0.38). The results of post hoc test further showed that the levels of PSD-95 (Fig. 9), Munc13 (Fig. 10), RIM1 (Fig. 11) and Rab3A (Fig. 12) in 1FG did not change significantly compared with those in CG (all P > 0.05). The levels of PSD-95, Munc13 and Rab3A in 3FG and 7FG were significantly higher than those in CG (P < 0.05, P < 0.01), RIM1 level showed an increasing trend compared with CG, but there was no significant difference (P > 0.05). The level of Munc13 in 3FG was significantly higher than that in 1FG (P < 0.01), and the levels of PSD-95, Munc13 and Rab3A in 7FG were significantly higher than that in 1FG (all P < 0.01).

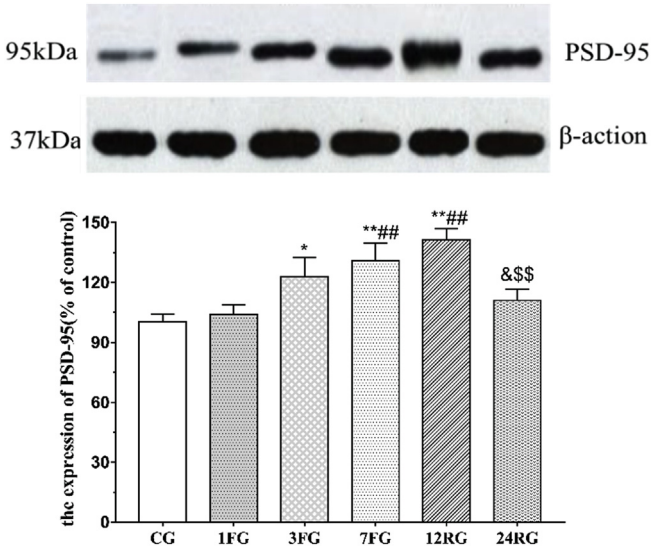

Fig. 9. Changes of PSD-95 protein levels in the striatum of rats in each group. Compared to CG, *:$P < 0.05$, **:$P < 0.01$; Compared to 1FG, #: $P < 0.05$, ##$P < 0.01$; Compared to 7FG, &:$P < 0.05$, &&:$P < 0.01$; Compared to 3FG, ^: $P < 0.05$, ^^: $P < 0.01$; Compared to 12RG, $: $P < 0.05$, $$: $P < 0.01$; (one-way analysis of variance).

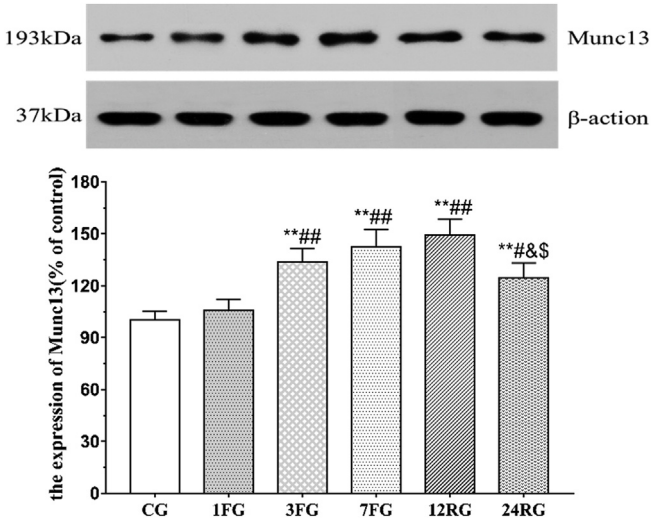

Fig. 10. Changes of Munc13 protein levels in the striatum of rats in each group.

Rab3A level in 7FG was also significantly higher than that in 3FG (P < 0.01). The levels of PSD-95, Munc13, RIM1 and Rab3A had still an increasing trend compared with 7FG, but there was no significant difference (P > 0.05), while there was significant difference compared with CG and 1FG (P < 0.05 or P < 0.01). The level of Rab3A in 12RG was also significantly different from that in 3FG (P < 0.01). The levels

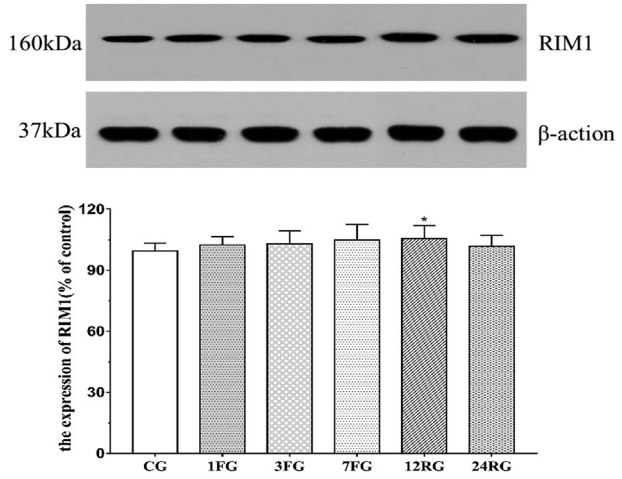

Fig. 11. Changes of RIM1 protein levels in the striatum of rats in each group.

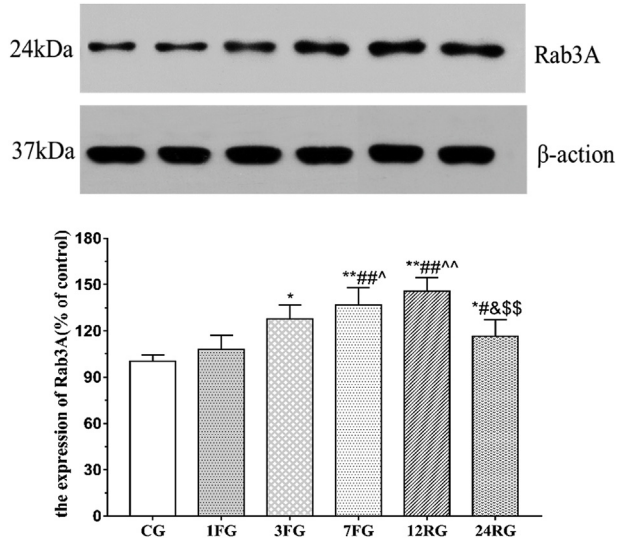

Fig. 12. Changes of Rab3A protein levels in the striatum of rats in each group.

of PSD-95, Munc13 and Rab3A in 24RG was significantly lower than those in 7FG (all $P < 0.05$), and significantly lower than those in 12RG ($P < 0.05$ or $P < 0.01$). Munc13 and Rab3A in 24RG were significantly lower than those in CG and 1FG ($P < 0.05$ or $P < 0.01$).

4. Discussion

4.1. Effect of exercise-induced fatigue on the behavior of rats

From the appearance, the rats had dark hair, sluggish eyes, and lacked appetite. Their limbs couldn't fully support their body weight, so they squatted on the ground, hind limb spacing widening; they also showed shortness of breath and tremor-like symptoms after exhaustive exercise. In addition, the body weight of the rats also decreased after repetitive exercise fatigue, indicating that exhaustive exercise caused an imbalance in the body's catabolism and anabolism, especially an enhanced catabolism, which will affect other physiological functions of rats in the long run. Subsequent behavioral experiments confirmed this hypothesis. The relative grip strength decreased, the retention time on the rotating rod decreased, indicating the rat's strength, balancing and coordinating function decreased, which are important manifestations of exercise fatigue (Gandevia, 2001; Masaaki and Yasuyoshi, 2012). With the prolongation of recovery time after fatigue, the rat's strength, balancing and coordinating function partly recovered, but couldn't return to normal after 24 h of exercise, suggesting that repetitive exercise fatigue involved (or damaged) the central motor control system of rats.

4.2. Effect of exercise-induced fatigue on asymmetric synaptic morphology in the striatum

A synapse is the main part of information transmission in the central nervous system. The synapses of the striatum can be divided into symmetrical and asymmetric synapses, among which the Glu synapses of striatum are asymmetric (Bamford et al., 2004; Kawaguchi, 1997; Izzo and Bolam, 1988). It has been reported that exercise fatigue can damage the Glu synaptic function in the hippocampus (Sun et al., 2017) and striatum (Ma et al., 2018) of rats, but whether this change is accompanied by abnormal changes in the synaptic structure is still uncertain. In this experiment, the ultrastructure of asymmetric synapses in rat striatum was observed by transmission electron microscopy. The results showed that the ultrastructure changes of striatum became more obvious with the accumulation of exercise-induced fatigue, the main manifestation were that the length of synaptic active zone of striatum, the thickness of PSD and the curvature of synaptic interface increased in different degrees. The change of synaptic cleft was not obvious. The results suggested that repetitive exercise fatigue could induce abnormal changes in the structure of striatum asymmetric synapses.

The presynaptic active zone is formed by transferring from precursor active zone to the putative presynaptic contact surface in the form of vesicle transport and then fusing with the plasma membrane (Ahmari et al., 2000). It is a presynaptic zone dedicated to the release of vesicles which can modulate optimal timing and speed of synaptic transmission, and it can also dynamically regulate the overall level, efficiency and reliability of transmitter release. The presynaptic active zone is between 200 and 300 nm in diameter (Schikorski and Stevens, 2001), and its area is closely related to the probability of transmitter release (Schikorski and Stevens, 1997). The smaller active zone indicates a lower probability of transmitter release (Kreitzer and Malenka, 2008). In addition, the curvature of curved synapses is higher than that of straight synapses. Generally speaking, the larger the curvature of synapse interface, the larger range of contact between presynaptic and postsynaptic membrane, and the stronger synaptic function. Therefore, studies have analyzed the plasticity of synapses from the perspective of the curvature change of synaptic interface (Dyson and Jones, 1980) and found that the length of presynaptic active zone and the curvature of synaptic interface of asymmetric synapses in rat striatum were significantly increased after exercise-induced fatigue. These results suggest that high intensity exercise can increase the probability of transmitters release and enhance the efficiency of synaptic transmission by increasing the length of synaptic active zone and the curvature of synaptic interface, thereby change synaptic plasticity, which is consistent with the electrophysiological results reported by Ma J et al. (Ma et al., 2018). After the release of neurotransmitters from the presynaptic active zone, they diffused through the synaptic gap and acted on the corresponding receptors on the postsynaptic membrane to complete the nerve information transmission. Therefore, the wider the synaptic gap, the longer it took for neurotransmitters to diffuse to the postsynaptic membrane, and the more neurotransmitters were reuptaken or decomposed. Therefore, it is generally believed that the increase in the width of the synaptic gap will lead to the reduction of synaptic transmission function, and vice versa. This experiment found that there was an increasing trend in the synaptic cleft of striatum asymmetric synapses after exercise-induced fatigue, but there was no significant change. This may be due to the fact that synaptic cleft is insensitive to high intensity exercise, and excessive enhancement of synaptic transmission is resisted only by its slight increase.

PSD is a homogeneous dense substance on the medial cytoplasmic surface of postsynaptic membrane, its components are mainly tubulin, actin, neurofilament protein and fodrin (de Bartolomeis and Fiore, 2004), it is the structural basis for postsynaptic signal transduction and

integration. The thickness of PSD is closely related to changes of synaptic function and is an important morphological index for synaptic plasticity. The thicker PSD becomes, the better communication between neurons gets. A decrease in the thickness of PSD indicates a decrease in the level of various proteins, which inevitably affects transmission of neurotransmitters (Thiel, 1993). In this experiment, it was found by electron microscopy that PSD showed a semicircular band with high electron density. The thickness of asymmetric synaptic PSD in rat striatum increased significantly after repetitive exercise-induced fatigue and decreased during recovery period which indicated that the plasticity of corticostriatal synaptic structure was impaired, and this further confirmed that exercise-induced fatigue can damage the synaptic plasticity of corticostriatal in a bidirectional manner reported by Ma J et al. (Ma et al., 2018).

4.3. Effects of exercise-induced fatigue on striatum asymmetric synaptic vesicles

Neurotransmitters are the physical basis of synaptic communication, especially in chemical synapses. Neurotransmitter release is mediated by synaptic vesicles, during which synaptic vesicles need to be transported to the synaptic active zone for the release of neurotransmitters. Therefore, the number of synaptic vesicles and their position relative to the synaptic active zone are closely related to synaptic function. In this study, the shortest distance between synaptic vesicles was used as an index to evaluate the accumulation of synaptic vesicles (Nikonenko and Skibo, 2004). The number of vesicles in the asymmetric synapses, the shortest distance between vesicles, and the size of the vesicles were observed through a transmission electron microscope. It was found that exercise-induced fatigue could not change the number and size of synaptic vesicles in rat striatum, but it could significantly change the spatial distribution of synaptic vesicles. Under normal conditions, the vesicles in the asymmetric synapses of rat striatum were dispersed, there were relatively less docking and circulating vesicles and more resting vesicle; but with the accumulation of exercise fatigue, the number of docking and circulating vesicles in the asymmetric synapses of the rat striatum increased, the shortest distance between them decreased, while resting vesicles decreased in number and the distance between them. The trend test results further showed that the synaptic vesicle ratio increased with the accumulation of exercise fatigue in the range of 200 nm from the asymmetric synaptic active zone of the rat striatum (Fig. 8, $P < 0.05$). The aggregation of synaptic vesicles at the front of the synapse was a significant feature of normal chemical synapses. Synaptic vesicles located in different areas had different releasability, and vesicles that accumulated in the synaptic active zone released more easily (Rizzoli and Betz, 2004). Therefore, the increase in the number of docking and circulating vesicles found in this study indicated that asymmetric synaptic vesicles in the striatum of rats released more easily after exercise-induced fatigue, which may be another mechanism leading to the enhancement of asymmetric synaptic function in the striatum of rats after exercise-induced fatigue.

4.4. Effects of exercise-induced fatigue on synaptic protein levels in striatum

RIM1 and Munc13, as two specific proteins in the presynaptic active zone, play an important role in the regulation of transmitter release and synaptic transmission efficiency (Varoqueaux et al., 2002; Schoch et al., 2002). Rab3A is an important protein expressed on synaptic vesicles, it can switch from the inactivation state of binding GDP to the activity state of binding GTP, and then mediate the release process of synaptic vesicles (Sakane et al., 2006). It has been proved that RIM1 and Munc13 can form a trimer with Rab3A that links synaptic vesicles to cytomatrix, and thereby positions synaptic vesicles near the presynaptic plasma membrane (Dulubova et al., 2005), and it can regulate neurotransmitters release and synaptic transmission intensity. The results of this experiment showed that the RIM1 level of rat striatum only increased after exercise fatigue, but the levels of Munc13 and Rab3A increased significantly. The results suggested that exercise fatigue may enhance synaptic transmission efficiency by increasing Munc13 and Rab3A protein levels in rat striatum, while RIM1 may not participate in the regulation of synaptic transmission efficiency in rat striatum by increasing protein level. It has been found that the regulation of RIM1 on synaptic transmission is mainly achieved by phosphorylation which mainly mediated by PKA (Castillo et al., 2002; Kaeser and Südhof, 2005). However, whether RIM1 phosphorylation is involved in this study needs further experimental confirmation. In addition to the asymmetric synapses of Glu in the striatum, there are symmetric synapses that can release GABA, DA and ACh (Bamford et al., 2004; Kawaguchi, 1997; Izzo and Bolam, 1988). Since RIM1, Munc13 and Rab3A exist in all chemical synaptic terminals, further research is needed to confirm whether the changes in the levels of RIM1, Munc13 and Rab3A detected by western blotting in this study can accurately reflect the changes in protein levels in asymmetric synapses.

PSD-95 is a structural anchoring protein which locates in the PSD of asymmetric synapses, it is an important regulator of synaptic strength and plasticity (Nezhadi et al., 2017; Nieto-Sampedro et al., 1982). Hu el al (Hu et al., 2009). found that running can change the dendritic structure and upregulate protein level of PSD-95 significantly in normal rats. The results of this experiment also showed that there was a significant increase in the level of PSD-95 in rat striatum after repetitive exercise-induced fatigue, which was correlated with thickness of PSD. The increased level of PSD-95 in rat striatum after exercise-induced fatigue is conductive to the interconnection of various signal molecules on the postsynaptic membrane and the clustering and localization of signal molecules in neurons, and then enhancing the ability of neurons to respond to neural signals. It is one of the important structural foundations for the enhancement of synaptic transmission efficiency. These results further confirm the report of Ma J et al. (Ma et al., 2018).

5. Conclusion

Exercise-induced fatigue can reduce the rats' strength, balancing and coordinating functions and change the morphological structure of asymmetric synapses, the spatial distribution of synaptic vesicles, and the levels of related synaptic proteins in the striatum. This change involves both the presynaptic and postsynaptic membrane, and can eventually lead to abnormal enhancement of asymmetric synaptic transmission. The results confirmed that the impaired asymmetric synaptic functions in the striatum of rats after exercise-induced fatigue might be associated with the abnormal changes of synaptic morphological structure and the levels of related synaptic proteins.

Conflicts of interest

The authors declared that they have no competing interests.

Acknowledgments

This study was supported by grants from the Natural Science Foundation of Shandong Province (ZR2016CL12, ZR2019MH12).

References

Ahmari, S.E., Buchanan, J., Smith, S.J., 2000. Assembly of presynaptic active zones from cytoplasmic transport packets. Nat. Neurosci. 3, 445–451.
Alloway, K.D., Lou, L., Nwabueze-Ogbo, F., Chakrabarti, S., 2006. Topography of cortical projections to the dorsolateral neostriatum in rats: multiple overlapping sensorimotor pathways. J. Comp. Neurol. 499, 33–48.
Aune, T.K., Ingvaldsen, R.P., Ettema, G.J., 2008. Effect of physical fatigue on motor control at different skill levels. Percept. Mot. Skills 106, 371–386.
Bai, X., Strong, R., 2014. Expression of synaptophysin protein in different dopaminergic cell lines. J. Biochem. Pharmacol. Res. 2, 185–190.
Bamford, N.S., Zhang, H., Schmitz, Y., Wu, N.P., Cepeda, C., Levine, M.S., Schmauss, C., Zakharenko, S.S., Zablow, L., Sulzer, D., 2004. Heterosynaptic dopamine

neurotransmission selects sets of corticostriatal terminals. Neuron 42, 653–663.
Carro, E., Trejo, J.L., Busiguina, S., Torres-Aleman, I., 2001. Circulating insulin-like growth factor I mediates the protective effects of physical exercise against brain insults of different etiology and anatomy. J. Neurosci. 21, 5678–5684.
Castillo, P.E., Schoch, S., Schmitz, F., Südhof, T.C., Malenka, R.C., 2002. RIM1alpha is required for presynaptic long-term potentiation. Nature 415, 327–330.
Chaudhuri, A., Behan, P.O., 2000. Fatigue and basal ganglia. J. Neurol. Sci. 179, 34–42.
Cotman, C.W., Berchtold, N.C., 2002. Exercise: a behavioral intervention to enhance brain health and plasticity. Trends Neurosci. 25, 295–301.
Dalbem, A., Silveira, C.V., Pedroso, M.F., Breda, R.V., Werne Baes, C.V., Bartmann, A.P., da Costa, J.C., 2005. Altered distribution of striatal activity-dependent synaptic plasticity in the 3-nitropropionic acid model of Huntington's disease. Brain Res. 1047, 148–158.
Davis, J.M., Bailey, S.P., 1997. Possible mechanisms of central nervous system fatigue during exercise. Med. Sci. Sport. Exerc. 29, 45–57.
Davis, J.M., Alderson, N.L., Welsh, R.S., 2000. Serotonin and central nervous system fatigue: nutritional considerations. Am. J. Clin. Nutr. 72 (2 Suppl. l), 573S–578S.
de Bartolomeis, A., Fiore, G., 2004. Postsynaptic density scaffolding proteins at excitatory synapse and disorders of synaptic plasticity: implications for human behavior pathologies. Int. Rev. Neurobiol. 59, 221–254.
DeLuca, J., Genova, H.M., Capili, E.J., Wylie, G.R., 2009. Functional neuroimaging of fatigue. Phys. Med. Rehabil. Clin 20, 325–337.
Di Filippo, M., Picconi, B., Tantucci, M., Ghiglieri, V., Bagetta, V., Sgobio, C., Tozzi, A., Parnetti, L., Calabresi, P., 2009. Short-term and long-term plasticity at corticostriatal synapses: implications for learning and memory. Behav. Brain Res. 199, 108–118.
Ding, J., Peterson, J.D., Surmeier, D.J., 2008. Corticostriatal and thalamostriatal synapses have distinctive properties. J. Neurosci. 28, 6483–6492.
Dulubova, I., Lou, X., Lu, J., Huryeva, I., Alam, A., Schneggenburger, R., Südhof, T.C., Rizo, J., 2005. A Munc13/RIM/Rab3 tripartite complex:from priming to plasticity? EMBO J. 24, 2839–2850.
Durieux, P.F., Schiffmann, S.N., de Kerchove d'Exaerde, A., 2012. Differential regulation of motor control and response to dopaminergic drugs by D1R and D2R neurons in distinct dorsal striatum subregions. EMBO J. 31, 640–653.
Dyson, S.E., Jones, D.G., 1980. Quantitation of terminal parameters and their inter-relationships in maturing centrla synapsed: a perspective for experimental studies. Brain Res. 183, 43–59.
Fernandes, J., Arida, R.M., Gomez-Pinilla, F., 2017. Physical exercise as an epigenetic modulator of brain plasticity and cognition. Neurosci. Biobehav. Rev. 80, 443–456.
Fowler, M.W., Staras, K., 2015. Synaptic vesicle pools: principles, properties and limitations. Exp. Cell Res. 335 (2), 150–156.
Franzone, J.S., Reboani, M.C., 1977. Stimulating action of hematoporphyrin on motor coordination and resistance to fatigue in rats. Arch. Sci. Med. 4, 403–406.
Gandevia, S.C., 2001. Spinal and supraspinal factors in human muscle fatigue. Physiol. Rev. 81, 1725–1789.
García-Junco-Clemente, P., Linares-Clemente, P., Fernández-Chacón, R., 2005. Active zones for presynaptic plasticity in the brain. Mol. Psychiatry 10, 185–200 image 131.
Güldner, F.H., Ingham, C.A., 1980. Increase in postsynaptic density material in optic target neurons of the rat suprachiasmatic nucleus after bilateral enucleation. Neurosci. Lett. 17, 27–31.
Hu, S., Ying, Z., Gomez-Pinilla, F., Frautschy, S.A., 2009. Exercise can increase small heat shock proteins (sHSP) and pre- and post-synaptic proteins in the hippocampus. Brain Res. 1249, 191–201.
Hu, Y., Liu, X., Qiao, D., 2015. Increased extracellular dopamine and 5-hydroxytryptamine levels contribute to enhanced subthalamic nucleus neural activity during exhausting exercise. Biol. Sport 32, 187–192.
Izzo, P.N., Bolam, J.P., 1988. Cholinergic synaptic input to different parts of spiny striatonigral neurons in the rat. J. Comp. Neurol. 269, 219–234.
Jones, D.G., Devon, R.M., 1978. An ultrastructural study into the effects of pentobarbitone on synaptic organization. Brain Res. 147, 47–63.
Kaeser, P.S., Südhof, T.C., 2005. RIM function in short- and long-term synaptic plasticity. Biochem. Soc. Trans. 33, 1345–1349.
Kawaguchi, Y., 1997. Neostriatal cell subtypes and their functional roles. Neurosci. Res. 27, 1–8.
Kobayashi, A., Parker, R.L., Wright, A.P., Brahem, H., Ku, P., Oliver, K.M., Walz, A., Lester, H.A., Miwa, J.M., 2014. lynx1 supports neuronal health in mouse dorsal striatum during aging:an ultrastructural investigation. J. Mol. Neurosci. 53, 525–536.
Kreitzer, A.C., Malenka, R.C., 2008. Striatal plasticity and basal ganglia circuit function. Neuron 60, 543–554.
Ma, J., Chen, H., Liu, X., Zhang, L., Qiao, D., 2018. Exercise-induced fatigue impairs bidirectional corticostriatal synaptic plasticity. Front. Cell. Neurosci. 12, 14.
Martella, G., Tassone, A., Sciamanna, G., Platania, P., Cuomo, D., Viscomi, M.T., Bonsi, P., Cacci, E., Biagioni, S., Usiello, A., Bernardi, G., Sharma, N., Standaert, D.G., Pisani, A., 2009. Impairment of bidirectional synaptic plasticity in the striatum of a mouse model of DYT1 dystonia: role of endogenous acetylcholine. Brain 132, 2336–2349.
Masaaki, Tanaka, Yasuyoshi, Watanabe, 2012. Supraspinal regulation of physical fatigue. Neurosci. Biobehav. Rev. 36, 727–734.
Meeusen, R., Watson, P., Hasegawa, H., Roelands, B., Piacentini, M.F., 2006. Central fatigue: the serotonin hypothesis and beyond. Sports Med. 36, 881–909.
Meeusen, R., Watson, P., Hasegawa, H., Roelands, B., Piacentini, M.F., 2007. Brain neurotransmitters in fatigue and overtraining. Appl. Physiol. Nutr. Metabol. 32, 857–864.
Milosevic, L., Gramer, R., Kim, T.H., Algarni, M., Fasano, A., Kalia, S.K., Hodaie, M., Lozano, A.M., Popovic, M.R., Hutchison, W.D., 2018. Modulation of inhibitory plasticity in basal ganglia output nuclei of patients with Parkinson's disease. Neurobiol. Dis. 124, 46–56.
Moore, R.D., Romine, M.W., O'connor, P.J., Tomporowski, P.D., 2012. The influence of exercise-induced fatigue on cognitive function. J. Sport Sci. 30, 841–850.
Nakagawa, S., Takeuchi, H., Taki, Y., Nouchi, R., Kotozaki, Y., Shinada, T., Maruyama, T., Sekiguchi, A., Iizuka, K., Yokoyama, R., Yamamoto, Y., Hanawa, S., Araki, T., Miyauchi, C.M., Magistro, D., Sakaki, K., Jeong, H., Sasaki, Y., Kawashima, R., 2016. Basal ganglia correlates of fatigue in young adults. Sci. Rep. 6, 21386.
Nezhadi, A., Esmaeili-Mahani, S., Sheibani, V., Shabani, M., Darvishzadeh, F., 2017. Neurosteroid allopregnanolone attenuates motor disability and prevents the changes of neurexin 1 and postsynaptic density protein 95 expression in the striatum of 6-OHDA-induced rats' model of Parkinson's disease. Biomed. Pharmacother. 88, 1188–1197.
Nieto-Sampedro, M., Bussineau, C.M., Cotman, C.W., 1982. Isolation, morphology, and protein and glycoprotein composition of synaptic junctional fractions from the brain of lower vertebrates: antigen PSD-95 as a junctional marker. J. Neurosci. 2, 722–734.
Nikonenko, A.G., Skibo, G.G., 2004. Technique to quantify local clustering of synaptic vesicles using single section data. Microsc. Res. Tech. 65, 287–291.
Paillé, V., Picconi, B., Bagetta, V., Ghiglieri, V., Sgobio, C., Di Filippo, M., Viscomi, M.T., Giampà, C., Fusco, F.R., Gardoni, F., Bernardi, G., Greengard, P., Di Luca, M., Calabresi, P., 2010. Distinct levels of dopamine denervation differentially alter striatal synaptic plasticity and NMDA receptor subunit composition. J. Neurosci. 30, 14182–14193.
Park, S.S., Park, H.S., Jeong, H., et al., 2019. Treadmill exercise ameliorates chemotherapy-induced muscle weakness and central fatigue by enhancing mitochondrial function and inhibiting apoptosis. Int Neurourol J 23 (Suppl. 1), S32–S39.
Partridge, J.G., Tang, K.C., Lovinger, D.M., 2000. Regional and postnatal heterogeneity of activity-dependent long-term changes in synaptic efficacy in the dorsal striatum. J. Neurophysiol. 84, 1422–1429.
Peters, A., 1991. The Fine Structure of the Nervous System: the Cells and Their Processes. Oxford University Press, New York, pp. 140–168.
Petzinger, G.M., Walsh, J.P., Akopian, G., Hogg, E., Abernathy, A., Arevalo, P., Turnquist, P., Vuković, M., Fisher, B.E., Togasaki, D.M., Jakowec, M.W., 2007. Effects of treadmill exercise on dopaminergic transmission in the 1-methyl-4-phenyl-1,2,3,6-tetrahydropyridine-lesioned mouse model of basal ganglia injury. J. Neurosci. 27, 5291–5300.
Picconi, B., Passino, E., Sgobio, C., Bonsi, P., Barone, I., Ghiglieri, V., Pisani, A., Bernardi, G., Ammassari-Teule, M., Calabresi, P., 2006. Plastic and behavioral abnormalities in experimental Huntington's disease: a crucial role for cholinergic interneurons. Neurobiol. Dis. 22, 143–152.
Picconi, B., Piccoli, G., Calabresi, P., 2012. Synaptic dysfunction in Parkinson's disease. Adv. Exp. Med. Biol. 970, 553–572.
Poldrack, R.A., Packard, M.G., 2003. Competition among multiple memory systems: converging evidence from animal and human brain studies. Neuropsychologia 41, 245–251.
Rizzoli, S.O., Betz, W.J., 2004. The structural organization of the readily releasable pool of synaptic vesicles. Science 5666, 2037–2039.
Ronesi, J., Lovinger, D.M., 2005. Induction of striatal long-term synaptic depression by moderate frequency activation of cortical afferents in rat. J. Physiol. 562, 245–256.
Rozas, G., Lopez-Martin, E., Guerra, M.J., Labandeira-Garcia, J.L., 1998. The overall rod performance test in the MPTP-treated-mouse model of Parkinsonism. J. Neurosci. Methods 83, 165–175.
Sakane, A., Manabe, S., Ishizaki, H., Tanaka-Okamoto, M., Kiyokage, E., Toida, K., Yoshida, T., Miyoshi, J., Kamiya, H., Takai, Y., Sasaki, T., 2006. Rab3 GTPase-activating protein regulates synaptic transmission and plasticity through the inactivation of Rab3. Proc. Natl. Acad. Sci. U.S.A. 103, 10029–10034.
Schikorski, T., Stevens, C.F., 1997. Quantitative ultrastructural analysis of hippocampal excitatory synapses. J. Neurosci. 17, 5858–5867.
Schikorski, T., Stevens, C.F., 2001. Morphological correlates of functionally defined synaptic vesicle populations. Nat. Neurosci. 4, 391–395.
Schoch, S., Castillo, P.E., Jo, T., Mukherjee, K., Geppert, M., Wang, Y., Schmitz, F., Malenka, R.C., Südhof, T.C., 2002. RIM1alpha forms a protein scaffold for regulating neurotransmitter release at the active zone. Nature 415, 321–326.
Secher, N.H., Quistorff, B., Dalsgaard, M.K., 2006. The muscles work, but the brain gets tired. Ugeskr Laeger 168, 4503–4506.
Shiflett, M.W., Balleine, B.W., 2011. Molecular substrates of action control in cortico-striatal circuits. Prog. Neurobiol. 95, 1–13.
Smith, Y., Raju, D.V., Pare, J.F., Sidibe, M., 2004. The thalamostriatal system: a highly specific network of the basal ganglia circuitry. Trends Neurosci. 27, 520–527.
Smith, Y., Villalba, R.M., Raju, D.V., 2009. Striatal spine plasticity in Parkinsons disease: pathological or not. Park. Relat. Disord. 15 (Suppl. 3), S156–S161.
Sun, L.N., Li, X.L., Wang, F., Zhang, J., Wang, D.D., Yuan, L., Wu, M.N., Wang, Z.J., Qi, J.S., 2017. High-intensity treadmill running impairs cognitive behavior and hippocampal synaptic plasticity of rats via activation of inflammatory response. J. Neurosci. Res. 95, 1611–1620.
Takakusaki, K., Saitoh, K., Harada, H., Kashiwayanagi, M., 2004. Role of basal ganglia-brainstem pathways in the control of motor behaviors. Neurosci. Res. 50, 137–151.
Thiel, G., 1993. Synapsin I, synapsin II, and synaptophysin: marker proteins of synaptic vesicles. Brain Pathol. 3, 87–95.
Thomson, K., Watt, A.P., Liukkonen, J., 2009. Differences in ball sports athletes speed discrimination skills before and after exercise induced fatigue. J. Sport. Sci. Med. 8, 259–264.
van Praag, H., Christie, B.R., Sejnowski, T.J., Gage, F.H., 1999. Running enhances neurogenesis, learning, and long-term potentiation in mice. Proc. Natl. Acad. Sci. U.S.A. 96, 13427–13431.
Varoqueaux, F., Sigler, A., Rhee, J.S., Brose, N., Enk, C., Reim, K., Rosenmund, C., 2002. Total arrest of spontaneous and evoked synaptic transmission but normal synaptogenesis in the absence of Munc13-mediated vesicle priming. Proc. Natl. Acad. Sci. U.S.A. 99, 9037–9042.

Voorn, P., Vanderschuren, L.J., Groenewegen, H.J., Robbins, T.W., Pennartz, C.M., 2004. Putting a spin on the dorsal-ventral divide of the striatum. Trends Neurosci. 27, 468–474.
Yin, H.H., Knowlton, B.J., 2006. The role of the basal ganglia in habit formation. Nat. Rev. Neurosci. 7, 464–476.
Yin, H.H., Knowlton, B.J., Balleine, B.W., 2006. Inactivation of dorsolateral striatum enhances sensitivity to changes in the action-outcome contingency in instrumental conditioning. Behav. Brain Res. 166, 189–196.
Zhai, S., Tanimura, A., Graves, S.M., Shen, W., Surmeier, D.J., 2018. Striatal synapses, circuits and Parkinson's disease. Curr. Opin. Neurobiol. 48, 9–16.
Zhang, X.L., Guariglia, S.R., McGlothan, J.L., Stansfield, K.H., Stanton, P.K., Guilarte, T.R., 2015. Presynaptic mechanisms of lead neurotoxicity: effects on vesicular release, vesicle clustering and mitochondria number. PLoS One 10, e0127461.